Nexus of Future Materials 2 (2025) 255-261

Nexus of Future Materials
https://nfmjournal.com/

Preparation and investigation of the radiation protection properties of borate glasses with enhanced PbO_2 and BaO content

Mohammad A. Imheidat[a,*], Samer E'layan Alawaideh[b]

[a] Department of Physics, Faculty of Science, Isra University, Amman 11622, Jordan
[b] Department of Chemistry, Faculty of Science, Isra University, Amman 11622, Jordan

Keywords:
Borate glasses
Rare earth oxide
Barium oxide
Attenuation coefficient
Phy-X software

Abstract

This research explores the synthesis and radiation attenuation characterization of borate glasses with different concentrations of BaO and PbO_2, and their applicability for radiation shielding. BaO and PbO_2 were introduced and greatly affected the density of the glasses, where the density rose between 4.550 and 5.161 g/cm². The mass attenuation coefficient (MAC) was evaluated, assessing the energy coming from the Eu-152 radioactive source with the Phy-X software. When the energy was at its minimum value of 0.122 MeV, the findings showed that the glass containing 20 mol% BaO and 19 mol% PbO_2 exhibited a MAC of 1.531 cm²/g, and the glass sample with 26 mol% BaO and 25 mol% PbO_2 had a MAC of 1.737 cm²/g. The linear attenuation coefficient (LAC) was investigated, and the outcomes demonstrated that the glass with high BaO and PbO_2 content possessed high LAC values at every level of energy. The findings of the half-value layer (HVL) revealed that the glasses behaved well in terms of absorbency at minimal energy. At 0.122 MeV, the HVL value was around 0.1 cm, and increased to 1.872–2.144 cm at 0.867 MeV. Ba26Er2 was the identifier for the glass sample (containing 26 mol% BaO and 25 mol% PbO_2) with the smallest HVL. The glasses' effective atomic number (Z_{eff}) was determined, with the findings indicating that the highest Z_{eff} value was recorded at 0.122 MeV, ranging from 54.28 to 59.23. The Z_{eff} showed a significant decline when the energy levels rose, falling by more than 50% when the energy levels dropped between 0.122 and 0.245 MeV.

1. Introduction

Glass has enormous significance in human life as it can be used for various applications. In our homes, glass can be utilized as cookware, bottles, and drinking glasses.Its application does not end in households, but extends to manufacturing, electronic innovations, research laboratories, and architecture. Depending on the fabrication procedures, glass offers advantageous properties such as transparency, thermal resistance, purity, and strength [1–3]. In medical arenas, the rays coming from UV sources could be dangerous to our eyes, and specific kinds of medical equipment emit such rays to which personnel may be exposed. Eye protection against such dangerous UV rays can be accomplished using specialized lenses made of glass**.** In the radiology units of hospitals, glasses are used to protect personnel and patients from excessive exposure to both X-rays and gamma radiation emitted from sophisticated radiation machines during patients' treatment [4–6]. Particularly in hospital radiology units, the use of these glasses is emphasized because of the damaging effects of highly penetrating gamma radiation.

* Corresponding author:
E-mail address: m.khamees@iu.edu.jo
Received 14 August 2025; Accepted 23 September 2025; Published 25 September 2025
https://nfmjournal.com/articles/34

Although gamma radiation is very useful in diagnostic imaging and cancer treatment, if not properly managed or shielded with protective materials such as glass, it can cause serious health problems such as breast cancer, radiation sickness, and genetic mutations [7–10]. Due to the important performance of glasses, particularly in hospitals for shielding harmful gamma rays, there is a clear need to improve some of their properties, such as the optical and radiation shielding parameters, for enhanced performance in radiation protection [11–14]. This improvement can be achieved by introducing certain metal oxides into a particular glass composition and adjusting their concentration to optimize these properties; for example, glasses made with boron (borate glasses) exhibit good chemical durability, mechanical and thermal stability, and structural strength [15–17]. Such glasses can be further improved by adding metal oxides like BaO. The capabilities of PbO_2 and BaO are widely recognized for improving the optical properties of glasses, including their resistance to UV rays, durability, refractive index, color control, and transparency [18–20]. Because of their high atomic number compared to B_2O_3, such metal oxides also improve the radiation shielding properties, since their large atomic numbers increase the overall density of the matrix, thereby enhancing the absorption coefficient of the glass system. The present research work will therefore assess the BaO–PbO_2–B_2O_3–Er_2O_3 glass system's ability to shield against radiation.

2. Materials and methods

1.2 Glasses' preparation

Several borate glasses reinforced with different ratios of BaO and PbO_2 were made utilizing the melt-quenching procedure and compounds of B_2O_3, BaO, PbO_2, and Er_2O_3 of excellent purity (>99%). Each glass sample included around 20 g of mixed oxides, as shown in **Table 1**. The weighed batches were melted in a platinum crucible at 1100 ± 10 °C for 1 h to ensure homogeneity. The melts were then poured onto a preheated stainless-steel plate and immediately pressed with another preheated plate to achieve uniform thickness (~2–3 mm). The cooling rate during quenching was approximately 10–15 °C/s. To relieve residual stresses, the glasses were transferred directly into an annealing furnace maintained at 400 °C, held for 2 h, and then cooled slowly to room temperature at a rate of ~2 °C/min. An image of assembled glasses is shown in **Fig. 1**.

To determine the density of the glasses, the notion of Archimedes was applied. This principle is expressed in equation 1:

$$\rho = \frac{W_a}{W_a - W_L} \times \rho_L \quad (1)$$

where w_a represents the glass's weight in air, and w_L is the glass's weight in liquid.

Table 1 shows that the prepared glasses' density increases from 4.550 to 5.161 g/cm^3 as the BaO and PbO_2 increase from 20 to 26 mol% and 19 to 25 mol%, respectively, whereas the B_2O_3 decreases from 59 to 47 mol%. The glasses' codes are Ba20Er2, Ba22Er2, Ba24Er2, and Ba26Er2, with each code reflecting the concentration of BaO.

Fig.1. Photographs of the prepared BaO–PbO_2–B_2O_3–Er_2O_3 glass samples with different BaO content.

Table 1. The chemical composition of the prepared glasses.

Glass Code	BaO	PbO_2	B_2O_3	Er_2O_3	Density (g/cm^3)
Ba20Er2	20	19	59	2	4.550
Ba22Er2	22	21	55	2	4.754
Ba24Er2	24	23	51	2	4.958
Ba26Er2	26	25	47	2	5.161

2.2 Characteristics of radiation shields

The Phy-X software was utilized to study the qualities of the glasses that guard against radiation. [21]. This program is employed to calculate and analyze the way that materials interact with radiation, which provides crucial defensive parameters in order to efficiently optimize and develop new radiation-protective materials. The linear attenuation coefficient (LAC, μ) is the first parameter for examining the glasses' radiation protection ability. An effective formula for describing the LAC for the glass sample is the Lambert–Beer law, namely:

$$I = I_0 e^{-\mu x} \quad (2)$$

where I and I_0 are respectively the intensity of the photons after and before the glass sample. If the LAC of a glass sample is known, we can simply determine that the LAC divided by the sample's density yields the mass attenuation coefficient (MAC), namely:

$$MAC = \frac{LAC}{density} \quad (3)$$

For a glass sample containing different components, then the MAC can be identified with the mixture rule:

$$MAC = \sum_i w_i (MAC)_i \quad (4)$$

where w_i is the weight fraction of the i-th component; for example, for the glass sample Ba20Er2 in our work, we can express the mixture role as:

$$(MAC)_{Ba20Er2} = w_{Ba}(MAC)_{Ba} + w_{Pb}(MAC)_{Pb} + w_B(MAC)_B + w_{Er}(MAC)_{Er} + w_O(MAC)_O \quad (5)$$

The absorber's thickness of specified composition required to reduce the radiation beam's intensity to half of what it started at is known as the half-value layer (HVL). Mathematically:

$$HVL = \frac{0.693}{LAC} \quad (6)$$

Similarly, we can define the tenth-value layer (TVL) as the protective material's thickness required to bring the radiation intensity down to 10% of its original value. This is known as the TVL, which can be represented by the following formula:

$$TVL = \frac{2.3}{LAC} \quad (7)$$

The inverse of the LAC is the mean free path (MFP):

$$MFP = \frac{1}{LAC} \quad (8)$$

3. Results and Discussion

The color changes in the glass samples show that as the amounts of BaO and PbO_2 increase, the glass becomes denser, as illustrated in **Fig. 1**. Sample Ba20Er2 which has the least density of 4.550 g/cm³, is more transparent than sample Ba26Er2 which has the highest density of 5.161 g/cm³, as well as the maximum moles of PbO_2 and BaO (26% and 25%, respectively). Generally, a decrease in the MAC increases as the incoming radiation's energy increases (**Fig. 2**). At 0.122 MeV, the MAC for each sample is as follows: sample Ba20Er2 = 1.531 cm²/g, sample Ba22Er2 = 1.605 cm²/g, sample Ba24Er2 = 1.673 cm²/g, and sample Ba26Er2 = 1.737cm²/g; these MAC values are clearly distinct at this level according to **Fig. 2**'s caption. The decrease in MAC is rapid as the energy increases between 0.122 and 0.245 MeV; for example, sample Ba20Er2 reduces from 0.325 from 1.531 cm²/g, sample Ba22Er2 from 1.605 to 0.336 cm²/g, sample Ba24Er2 from 1.673 to 0.347 cm²/g, and sample Ba26Er2 from 1.737 to 0.357 cm²/g. At the highest energy level, that is 0.867 MeV, the MAC converges, indicating that all the samples have approximately the same attenuation ability, although sample Ba26Er2 has the highest attenuation strength at lower energies because of the large proportion of high-Z components in its composition.

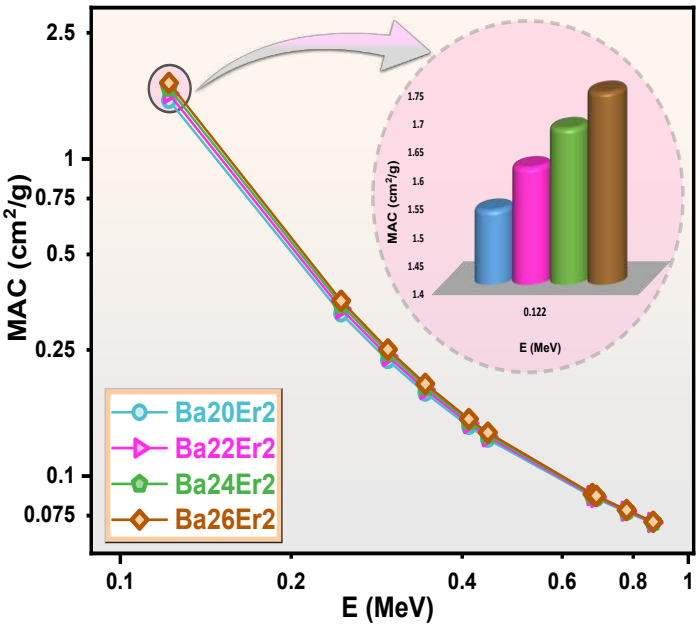

Fig.2. Mass attenuation coefficient (MAC) of the BaO–PbO_2–B_2O_3–Er_2O_3 glasses as a function of photon energy (0.1–1 MeV).

Fig. 3 illustrates the LAC values regarding the current glasses. All of the studied glasses have the highest LAC value at 0.122 MeV, with sample Ba26Er2 featuring the greatest LAC (8.962 cm^{-1}) due to its high content of BaO and PbO_2 (26 mol% and 25 mol%, respectively), while the sample with the lowest LAC is Ba20Er2, which has a low amount of BaO and PbO_2 (20 mol% and 19 mol%, respectively).

Overall, as the radiation energy level rises, the LAC falls, and we observed a significant decrease when the energy rises between 0.122 and 0.245 MeV due to an increase in the likelihood of photoelectric interaction, whereby sample Ba20Er2 decreases from 6.964 to 1.479 cm^{-1}, sample Ba22Er2 from 7.628 to 1.600 cm^{-1}, sample Ba24Er2 from 8.295 to 1.721 cm^{-1}, and sample Ba26Er2 from 8.962 to 1.842 cm^{-1}. The decrease in LAC becomes smooth on increasing the energy further; for example, at the highest energy level of 0.867 MeV, the LAC value of sample Ba20Er2 is 0.323 cm^{-1}, which is the lowest LAC at this energy, while sample Ba26Er2 decreases to 0.370 cm^{-1}, which is the maximum LAC at this energy, as depicted in **Fig. 3**.

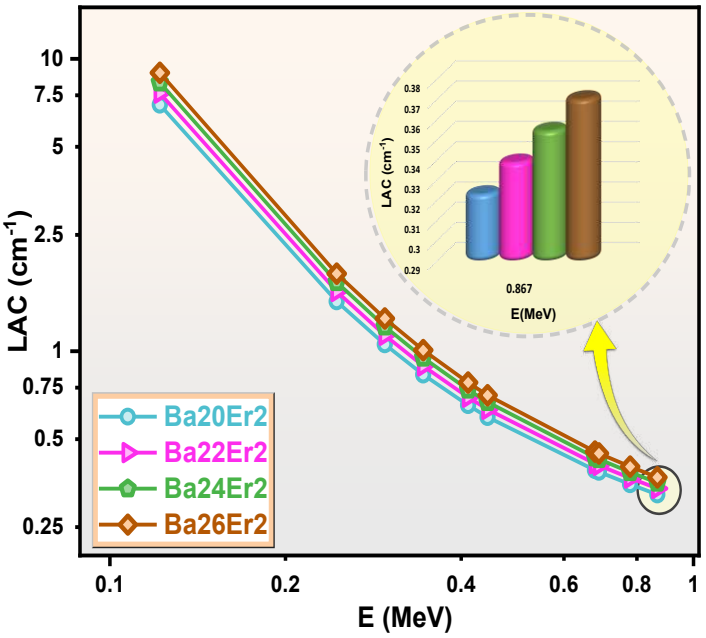

Fig.3. Linear attenuation coefficient (LAC) of the BaO–PbO_2–B_2O_3–Er_2O_3 glasses versus photon energy.

Consistently, sample Ba26Er2 because of its high-Z atom concentration within its composition displays the maximum LAC, suggesting increased defensive ability compared to the remaining samples of glass. The glasses' HVLs are depicted in **Fig. 4**. At the energy level of 0.122 MeV, sample Ba20Er2 has the highest thickness required to shield half of the intensity (0.100 cm) of the radiation, due to a lower interaction between the radiation and a lower amount of high-Z atoms in its structure. With an increase in the mole percentage concentration of PbO_2 and BaO, the HVL value decreases, with sample Ba26Er2 in **Fig. 4** possessing an HVL value of 0.077 cm that is the minimum at the energy level of 0.122 MeV, whereas the sample with the greatest HVL value is Ba20Er2. As we increase the energy of the radiation between 0.122 and 0.867 MeV, the HVL rises generally for every glass that was examined, as depicted in **Fig. 4**, and with a wide variation of HVLs. Sample Ba20Er2 rises from 0.100 to 2.144 cm, sample Ba22Er2 from 2.045 cm to 0.091 cm, sample Ba24Er2 from 1.954 to 0.084, and sample Ba26Er2, which persistently shows a lower HVL because of the high concentration of BaO and PbO_2 (26% and 25%, respectively), rises from 0.077 to 1.872 cm, demonstrating improved shielding capabilities at all energy levels.

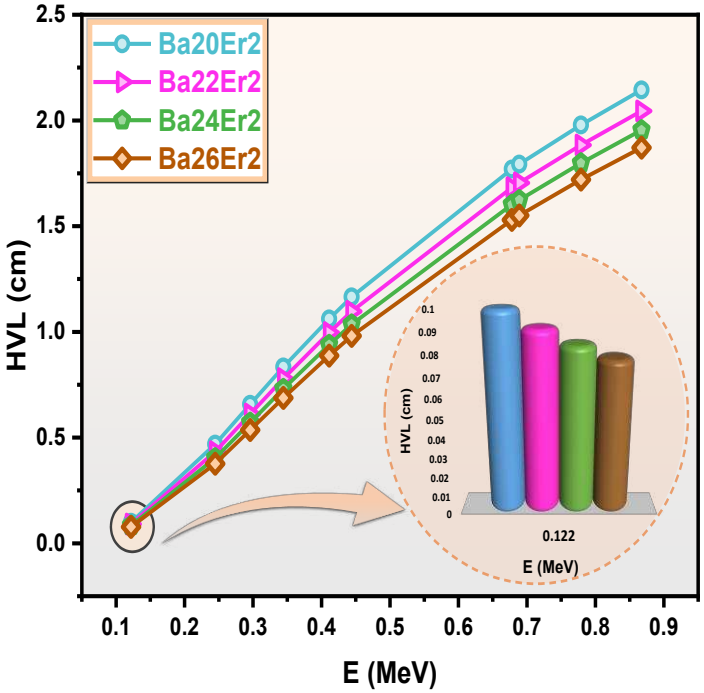

Fig.4. Half-value layer (HVL) as a function of photon energy.

In **Fig. 5**, we graphically represent the prepared glasses' MFP. The lowest MFP across every glass sample was obtained at 0.122 MeV using the Ba26Er2 specimen, having an MFP value of 0.112 cm, followed by sample Ba24Er2 with an MFP value of 0.121 cm, then sample Ba22Er2 with an MFP value of 0.131 cm, and lastly sample Ba20Er2 with the greatest MFP value (0.144 cm) at this level of energy. Since photoelectric contact is more likely to occur when energy rises between 0.122 and 0.245 MeV, all of the studied glasses' MFP values show a notable increase; for example, sample Ba20Er2 rises between 0.144 and 0.676 cm, showing the maximum increment, while sample Ba26Er2 increases from 0.112 to 0.543 cm, which has the lowest increment among every glass sample displayed in **Fig. 5**. As we further increase the energy between 0.245 and 0.867 MeV, there is a noticeable rise in the MFP for the present samples; for example, sample Ba20Er2 increases from 0.676 to 3.093 cm—this is the highest growth in the MFP value, which results due to the low content of BaO and PbO_2 (20 and 19 mol%, in that order) in its chemical composition, allowing for a deeper penetration of the radiation—whereas sample Ba26Er2 rises between 0.543 and 2.700 cm and thus has the lowest increase in MFP value because of the high amount of BaO and PbO_2 (26 mol% and 25 mol%, respectively) and higher interaction between the radiation and the high-Z atoms in its composition, making it the best material for shielding radiation. According to **Fig. 5**, raising the amount of BaO and PbO_2 and decreasing the B_2O_3 in the prepared glasses contributes to a lower MFP.

In **Fig. 6**, the glasses' effective atomic number (Z_{eff}) is displayed. As expected, the highest Z_{eff} values of every glass sample are obtained with the least amount of radiation energy (0.122 MeV), and then generally decrease as we increase the energy of the radiation. As an illustration, at 0.122 MeV sample Ba26Er2 has the highest Z_{eff} (59.23) due to its composition's elevated mole percentage of PbO_2 and BaO (26% and 25%, respectively); however, sample Ba20Er2 has the lowest Z_{eff} value (54.28) at this level of energy. The Z_{eff} values drop drastically as the energy increases between 0.122 and 0.245 MeV, with sample Ba20Er2 showing the highest decrease in Z_{eff} from 54.28 to 31.23, while sample Ba26Er2 exhibits the least amount of decline, going from 59.23 to 37.37. Continuing to raise the energy between 0.245 and 0.867 MeV, the Z_{eff} values decrease gradually for every glass that was examined. Glass sample Ba20Er2 decreases from 31.23 to 15.64, while sample Ba26Er2 decreases from 37.37 to 18.90, showing a higher shielding ability than the remaining glass samples.

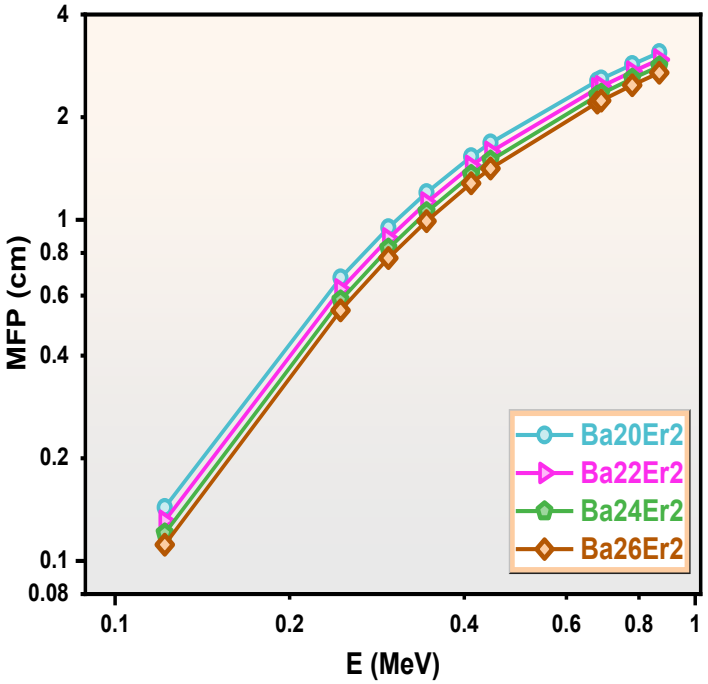

Fig.5. Mean free path (MFP) of the glass samples as a function of photon energy.

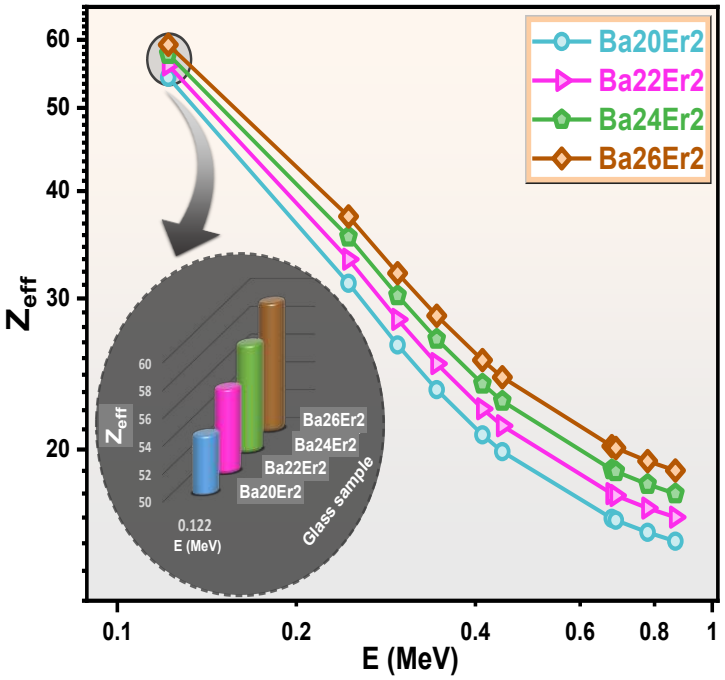

Fig.6. Effective atomic number (Z_{eff}) of the BaO–PbO_2–B_2O_3–Er_2O_3 glasses versus photon energy. The Z_{eff} decreases with energy, consistent with reduced photoelectric dominance.

The relationship between the HVL and the density for glasses is seen in **Fig. 7** at 0.444 MeV, with the figure showing that the glass samples' density and HVL have an inverse connection. Sample Ba20Er2 with the highest HVL (1.165 cm) has the lowest density (4.550 g/cm³). Then, the density reaches 4.754 g/cm³ for sample Ba22Er2, where the HVL decreases to 1.097 cm. Sample Ba24Er2 with a density of 4.958 g/cm³ has an HVL value of 1.035 cm, while sample Ba26Er2 has the highest density of 5.161 g/cm³, with the lowest HVL of 0.981. Therefore, the higher the density, the better the glass's shielding ability.

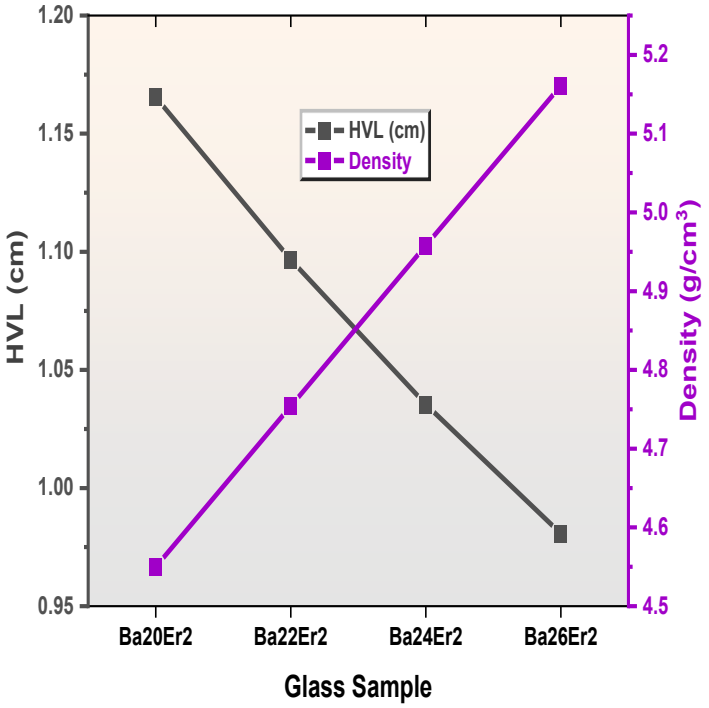

Fig.7. Correlation between the half-value layer (HVL) and density for the prepared glasses.

Fig. 8 and **Fig. 9** show the Z_{eff} for Ba20Er2 and Ba26Er2, respectively, at some selected energy levels. Generally, the Z_{eff} values decrease because the radiation's energy level has risen. The highest Z_{eff} value (54.28) was obtained at 0.122 MeV, and as **Fig. 8** shows, the Z_{eff} values drop sharply between 54.28 and 32.23 because of the high chances of photoelectric interaction between 0.122 and 0.245 MeV when the energy increases. Because of another energy gain between 0.245 and 0.678 MeV, the Z_{eff} value starts to gradually decline, decreasing from 31.23 to 16.63. The Z_{eff} value of 59.23 for sample Ba26Er2 is the most significant (see **Fig. 9**) at 0.122 MeV due to its high content of atoms with high atomic number (BaO and PbO_2). There is a sharp decrease in the Z_{eff} value when the energy reaches 0.245 MeV, which decreases from 59.23 to 37.37 and continues to decrease as we increase the energy, although not as rapidly as before; for instance, as the energy rises between 0.245 and 0.678 MeV, the Z_{eff} decreases between 37.37 and 20.18. Sample Ba26Er2 shows the least decrease in Z_{eff}, which makes it the greatest material for safeguarding against radiation. Our results are aligned with data from recent reports, which show enhanced attenuation at low photon energies due to the dominance of photoelectric absorption and increased matrix density [22-37]. In addition, our glasses deliver competitive low-energy attenuation while maintaining a simple borate base and introducing Er_2O_3 as a dual-purpose (structural/optical) high-Z additive. This positions Ba26Er2 as a practical composition for compact gamma radiation shielding where minimal thickness is required, while the graded set (Ba20Er2–Ba26Er2) provides tunable density–HVL trade-offs relevant to window or barrier design.

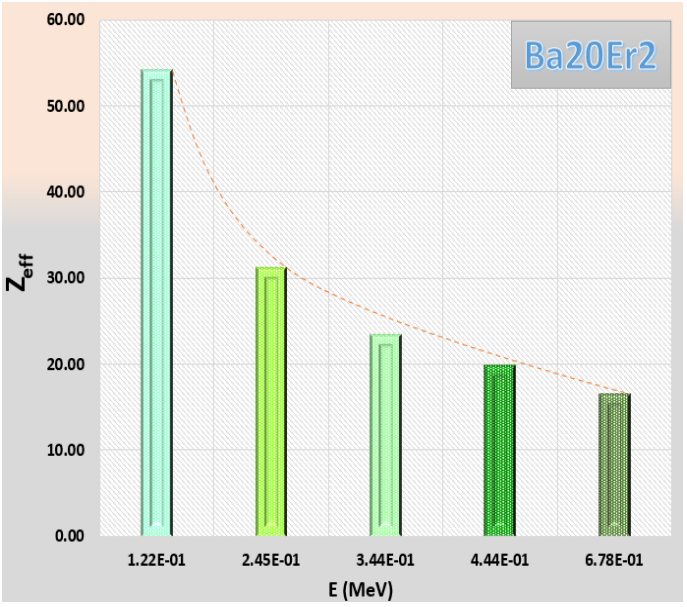

Fig.8. Effective atomic number (Z_{eff}) of the Ba20Er2 glass at selected photon energies.

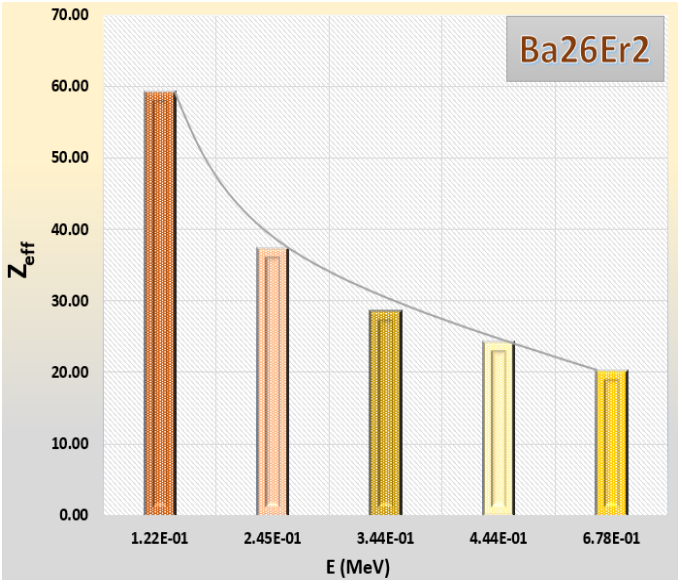

Fig.9. Effective atomic number (Z_{eff}) of the Ba26Er2 glass at selected photon energies.

Conclusion

This study investigated the preparation and radiation-protecting qualities of new borate glasses with various BaO and PbO_2 content, as well as their potential use for radiation protection. There was a significant effect on the density of the glasses from the addition of BaO and PbO_2, which increased from 4.550 to

5.161 g/cm³. Several attenuation factors were calculated by employing the Phy-X software at selected energy levels emitted by the Eu-152 radioactive source. As the energy level decreased to 0.122 MeV, the glass specimen containing 20 mol% BaO and 19 mol% PbO_2 displayed a MAC of 1.531 cm²/g, while the glass sample with 26 mol% BaO and 25 mol% PbO_2 had a MAC of 1.737 cm²/g. The LAC results showed that glasses with higher concentrations of PbO_2 and BaO exhibited higher LAC values across all energies. According to the HVL data, the glasses performed well at low energy in terms of attenuation. The HVL value at 0.122 MeV was approximately 0.1 cm, while at 0.867 MeV it rose to 1.872–2.144 cm. The glass sample with the lowest HVL was Ba26Er2, which comprised of 26 mol% BaO and 25 mol% PbO_2. The Z_{eff} of the glasses were calculated, and the results revealed that the greatest values, ranging from 54.28 to 59.23, were observed at 0.122 MeV. When the energy level increased, the Z_{eff} showed a notable decline; specifically, it decreased by over 50% when the energy increased from 0.122 to 0.245 MeV.

The results obtained in this work show that our glasses are promising candidates for use in medical imaging, nuclear facilities, and protective viewing windows, offering transparent and lead-reduced alternatives. Future work will test their performance at higher gamma energies, evaluate the long-term durability under irradiation, and explore the optical potential of Er2O3 for multifunctional applications.

References

[1] A. Saleh, Comparative shielding features for X/Gamma-rays, fast and thermal neutrons of some gadolinium silicoborate glasses, Progress in Nuclear Energy, 154 (2022) 104482.

[2] R. Bagheri, A. Khorrami Moghaddam, H. Yousefnia, Gamma ray shielding study of barium–bismuth–borosilicate glasses as transparent shielding materials using MCNP-4C code, XCOM program, and available experimental data, Nuclear Engineering and Technology, 49 (2017) 216-223.

[3] A. Acikgoz, G. Demircan, D. Yılmaz, B. Aktas, S. Yalcin, N. Yorulmaz, Structural, mechanical, radiation shielding properties and albedo parameters of alumina borate glasses: Role of CeO2 and Er2O3, Materials Science and Engineering B, 276 (2022) 115519.

[4] A.H. Almuqrin, K. Mahmoud, U. Rilwan, M. Sayyed, Influence of various metal oxides (PbO, Fe2O3, MgO, and Al2O3) on the mechanical properties and γ-ray attenuation performance of zinc barium borate glasses, Nuclear Engineering and Technology, 56 (2024) 2711-2717.

[5] M. Zubair, E. Ahmed, D. Hartanto, Comparison of different glass materials to protect the operators from gamma-rays in the PET using MCNP code, Radiation Physics and Chemistry, 190 (2021) 109818.

[6] I. Geidam, K. Matori, M. Halimah, K. Chan, F. Muhammad, M. Ishak, S. Umar, Oxide ion polarizabilities and gamma radiation shielding features of TeO2–B2O3–SiO2 glasses containing Bi2O3 using Phy-X/PSD software, Materials Today Communications, 31 (2022) 103472.

[7] M. Pacheco, M. Gibin, M. Silva, G. Montagnini, R. Viscovini, A. Steimacher, F. Pedrochi, V. Zanuto, R. Muniz, BaO–reinforced SiO2–Na2O–Ca(O/F2)–Al2O3 glasses for radiation safety: On the physical, optical, structural and radiation shielding properties, Journal of Alloys and Compounds, 960 (2023) 171019.

[8] B. Aktas, A. Acikgoz, D. Yilmaz, S. Yalcin, K. Dogru, N. Yorulmaz, The role of TeO2 insertion on the radiation shielding, structural and physical properties of borosilicate glasses, Journal of Nuclear Materials, 563 (2022) 153619.

[9] L. Srinivasa Rao, S. Hussain, A. Navalika, B. Chennakesava Rao, T. Venkatappa Rao, F.C. Hila, Effect of ZnO nanoparticles on physical, optical and radiation shielding properties of Bi2O3-B2O3-Cr2O3 glasses, Results in Optics, 12 (2023) 100491.

[10] H. Karami, V. Zanganeh, M. Ahmadi, Study nuclear radiation shielding, mechanical and acoustical properties of TeO2-Na2O-BaO-TiO2 alloyed glasses, Radiation Physics and Chemistry, 208 (2023) 110917.

[11] R. Rajaramakrishna, W. Chaiphaksa, S. Kaewjaeng, S. Kothan, J. Kaewkhao, Study of radiation shielding and luminescence properties of 1.5 μm emission from Er3+ doped zinc yttrium borate glasses, Optik, 289 (2023) 171273.

[12] B. Aktas, A. Acikgoz, D. Yilmaz, S. Yalcin, K. Dogru, N. Yorulmaz, The role of TeO2 insertion on the radiation shielding, structural and physical properties of borosilicate glasses, Journal of Nuclear Materials, 563 (2022) 153619.

[13] B. Guven, E. Ercenk, S. Yilmaz, Investigation of radiation shielding properties of basalt-based glasses: Binodal/Spinodal decomposition effect theory, Progress in Nuclear Energy, 163 (2023) 104810.

[14] A.H. Almuqrin, M. Rashad, C.V. More, M. Sayyed, M. Elsafi, An experimental and theoretical study to evaluate Al2O3–PbO–B2O3–SiO2–BaO radiation shielding properties, Radiation Physics and Chemistry, 222 (2024) 111824.

[15] J. Wu, J. Hu, Z. Deng, Y. Feng, H. Fan, Z. Wang, K. Wang, Q. Chen, W. Zhang, Comparative investigation of physical, X-ray and neutron radiation shielding properties for B2O3-MnO2-CdO borate glasses, Ceramics International, 49 (2023) 30915-30923.

[16] K. Mariselvam, J. Liu, Concentration effect of Tm3+ ions doped B2O3-Li2CO3-BaCO3-CaF2-ZnO glasses: Blue laser and radiation shielding investigations, Optics and Laser Technology, 154 (2022) 108262.

[17] K. Hanamar, G. Hiremath, B. Hegde, N. Ayachit, N. Badiger, Effect of the samarium on the mechanical and radiation shielding capabilities of lead-free zinc-borate-lithium glasses, Optik, 273 (2023) 170397.

[18] S. Kaewjaeng, N. Chanthima, J. Thongdang, S. Reungsri, S. Kothan, J. Kaewkhao, Synthesis and radiation properties of Li2O-BaO-Bi2O3-P2O5 glasses, Materials Today Proceedings, 43 (2020) 2544-2553.

[19] N. Chanthima, J. Kaewkhao, P. Limkitjaroenporn, S. Tuscharoen, S. Kothan, M. Tungjai, S. Kaewjaeng, S. Sarachai, P. Limsuwan, Development of BaO–ZnO–B2O3 glasses as a radiation shielding material, Radiation Physics and Chemistry, 137 (2017) 72-77.

[20] A.S. Altowyan, M. Sayyed, A. Kumar, M. Rashad, SrO–ZnO–PbO–B2O3 glassy insights: Unveiling the structural and optical features for gamma ray shielding efficacy, Optical Materials, 152 (2024) 115534.
[21] E. Şakar, Ö.F. Özpolat, B. Alım, M. Sayyed, M. Kurudirek, Phy-X/PSD: Development of a user friendly online software for calculation of parameters relevant to radiation shielding and dosimetry, Radiation Physics and Chemistry, 166 (2019) 108496.
[22] R.M. Hamad, M.K. Hamad, N. Dwaikat, Assessment of FexSe0.5Te0.5 alloy properties for ionizing radiation shielding applications: An experimental study, Applied Physics A, 128 (2022) 574.
[23] Y. Alajerami, M. Mhareb, M. Sayyed, M. Hamad, E. Abuelhia, A. Alshamari, M.Y. Alqahtani, M.A. Imheidat, Physical and radiation shielding properties for borate, boro-tellurite, and tellurite glass system modified with different modifiers: Comparative study, Optical Materials, 147 (2023) 114558.
[24] Y.S.M. Alajerami, M.A. Morsy, M.H.A. Mhareb, Structural, optical, and radiation shielding features for a series of borate glassy system modified by molybdenum oxide, European Physical Journal Plus, 136 (2021) 583.
[25] M. Mhareb, M.K. Hamad, A. Alshamari, M. Sayyed, N. Dwaikat, Experimental radiation shielding, mechanical and optical properties for borosilicate glass system: Role of varying SrO, Radiation Physics and Chemistry, 221 (2024) 111762.
[26] R. Hamad, M.K. Hamad, M. Mhareb, M. Sayyed, Y. Alajerami, N. Dwaikat, M. Almessiere, M.A. Imheidat, K.A. Ziq, Structural and radiation shielding features for BaSn1-xZnxO3 perovskite, Physica B: Condensed Matter, 638 (2022) 413925.
[27] M.K. Hamad, Evaluation of photon shielding properties for new refractory tantalum-rich sulfides Ta9(XS3)2 alloys: A study with the MCNP-5, Annals of Nuclear Energy, 184 (2023) 109687.
[28] M.K. Hamad, Effects of bismuth substitution on the structural and ionizing radiation shielding properties of the novel BaSn1-xBixO3 perovskites: An experimental study, Materials Chemistry and Physics, 308 (2023) 128254.
[29] M.K. Hamad, Effect of WO3 on structural, optical, mechanical, and ionizing radiation shielding properties of borate-tellurite glass network, Ceramics International, 51 (2025) 9763-9771.
[30] M.K. Hamad, Enhancing ionizing radiation shielding properties with PbO and ZnO substitutions in B2O3–BaO–TiO2 novel glass system, Radiation Physics and Chemistry, 229 (2025) 112499.
[31] M.K. Hamad, On the ionizing radiation protection properties of different chromium-based alloys: A study with the Geant4 Monte Carlo toolkit, Annals of Nuclear Energy, 213 (2025) 111134.
[32] E.A. Farrag, M.K. Hamad, A. Ali, A. Abdelmonem, H. Al-Taani, Unveiling the shielding potential: Exploring photon and neutron attenuation in a novel lead-free XCr2Se4 chalcogenide spinel alloys with MCNP 4C code, Radiation Physics and Chemistry, 226 (2024) 112337.
[33] H. Al-Taani, M.K. Hamad, Enhanced radiation shielding performance of novel glass compositions: A comprehensive analysis of gamma and neutron attenuation properties, Radiation Physics and Chemistry, 237 (2025) 112987.
[34] T. Ghrib, A.B. Ali, F. Ercan, M. Mhareb, S. Al-muteliq, I. Ercan, O. Kaygili, M. Hamad, N. Sfina, M. Mhiri, M. Alqahtani, M. Younas, Structural, optical, photoluminescence and radiation-shielding investigation of magnesium doped barium zirconate (BaZrO3) ceramics, Radiation Physics and Chemistry, 223 (2024) 111976.
[35] Y. Slimani, M.H.A. Mhareb, M.K. Hamad, Radiation shielding, structural, and optical properties for YBa2Cu3O7-d ceramic doped with TiO2 irradiated by different doses, Arabian Journal for Science and Engineering, 50 (2025) 541-549.
[36] Y. Slimani, M. Mhareb, M.K. Hamad, I. Alrammah, A. Thakur, Preparation, characterization, and study of radiation shielding performance of YBa2Cu3Oy/WO3 ceramics exposed to different gamma rays doses, Journal of the Indian Chemical Society, 101 (2024) 101479.
[37] Y. Haddad, M.K. Hamad, G. Sattonnay, Pure rare earth oxides as high-performance gamma, neutron, and charged particles shielding materials: A comparative study of Ho2O3, Er2O3, Yb2O3, and Y2O3, Materials Chemistry and Physics, 347 (2025) 131440.